

# Hydrothermal Synthesis of Metal Oxide Nano- and Microparticles in Supercritical Water

V. I. Anikeev

Boreskov Institute of Catalysis, Siberian Division, Russian Academy of Sciences, Novosibirsk

e-mail: anik@catalysis.ru

Received March 29, 2010

**Abstract**—Hydrothermal syntheses of nano- and microparticles of metal oxides of two types,  $\text{LiMO}_n$  ( $\text{LiCoO}_2$ ,  $\text{LiNiO}_2$ ,  $\text{LiZnO}_2$ , and  $\text{LiCuO}_2$ ) and  $\text{MO}_n$  ( $\text{Ga}_2\text{O}_3$ ,  $\text{CeO}_2$ ) were performed under continuous conditions in a tubular reactor with the use of supercritical water. An important role in the synthesis of nanoparticles and the reproducibility of the results was played by the conditions of mixing of supercritical water and precursor solution flows. The morphology and composition of synthesized compounds were studied by scanning electron microscopy and X-ray diffraction. The syntheses of  $\text{LiCoO}_2$ ,  $\text{LiNiO}_2$ ,  $\text{LiZnO}_2$ ,  $\text{LiCuO}_2$ ,  $\text{Ga}_2\text{O}_3$ , and  $\text{CeO}_2$  were most successful.

**Keywords:** hydrothermal synthesis, metal oxide nano- and microparticles, supercritical water.

**DOI:** 10.1134/S0036024411030034

## INTRODUCTION

Many methods were suggested for the synthesis of nanostructured materials, such as nanoparticles, nanofilms, and nanowires. These methods can be divided into two main groups: (1) the production of nanostructures from bulk materials and (2) the production of nanostructures from molecular level systems.

Supercritical fluids are an attractive medium for the synthesis, modification, and formation of (in)organic material nanoparticles [1–4]. Such nanostructures and materials exhibit unusual properties different from those of massive materials. Supercritical fluids are extensively used for the preparation of inorganic material nanoparticles (metals (Pt, Pd, Rh, Au, Ag, etc.) and their composites, metal oxides and nitrides ( $\text{TiO}_2$ ,  $\text{Cr}_2\text{O}_3$ ,  $\text{Co}_2\text{N}$ , and  $\text{Cr}_2\text{N}$ ) [3]),  $\text{LiFePO}_4$ -type metal oxide (used as materials for cathodes in Li cells) and similar compound nanoparticles [4], and for the microencapsulation of inorganic nanoparticles in polymer coatings.

Metals and their oxides in the form of nanoparticles having chemical, thermal, optical, magnetic, and other properties different from those of their massive analogues are extensively used in catalysis, medicine, electronics, etc. The applicability range of nanoparticles in many respects depends not only on their properties, such as size, structure, and morphology, but also on the method used for their preparation. The nanosize of a material is determined by one of its dimensions (diameter or thickness), which change from 1 to 200 nm.

Metal and/or metal oxide nanoparticles deposited on a surface are of considerable interest for applications because of their unique properties determined by metal morphology, dispersity, and concentration on the surface. For instance, nanoparticles with a high specific surface area deposited on various substrates are used as catalysts of various chemical transformations. Depending on the selected materials and supercritical fluid, nanoparticles can be produced by the chemical method, the method of rapid expansion of supercritical solution (RESS), gas anti-solvent processes (the GaSR, GASP, SAS, PCA, and SEDS variants), processes of particle preparation from gas-saturated solutions (PGST<sup>TM</sup>) [2], the hydrothermal synthesis method [2, 5], and the method of reverse micelles. The selection of a method for synthesizing nanoparticles is determined by particular purposes.

Among the suggested methods for the synthesis of metal, metal oxide, and metal hydroxide nanoparticles, hydrothermal synthesis methods [5–7] in supercritical water are most advantageous and promising. Several main one- and multistage reactions of precursors and metal salts can be used in the synthesis of particles in supercritical water, including hydrolysis, dehydration, thermolysis, reduction, and oxidation (as a rule, in the presence of hydrogen). In the region of critical water parameters, the dissociation of water and, therefore, the concentrations of  $\text{H}^+$  and  $\text{OH}^-$  ions increase. As a result, the hydrothermal synthesis of metal oxide nanoparticles from metal salts is per-

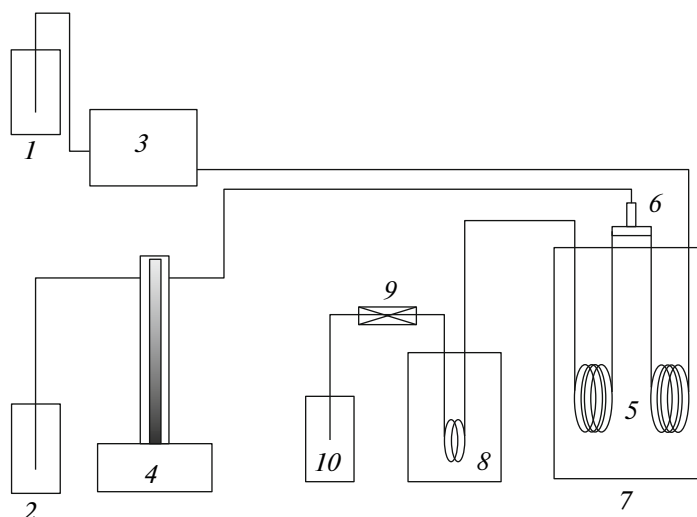
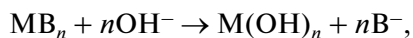


**Fig. 1.** Unit with a tubular reactor for the hydrothermal synthesis of nanoparticles: 1, 2, vessels for water and reagents; 3, piston pump; 4, syringe pump; 5, tubular reactor; 6, mixer; 7, furnace with a boiling sand layer; 8, refrigerator; 9, back pressure regulator; and 10, vessel for synthesized products.

formed in supercritical water in two-stage hydrolysis and dehydration reactions,



Hydrothermal transformations of metal salts (nitrates and sulfates) in supercritical water were performed to synthesize  $\text{Fe}_2\text{O}_3$ ,  $\text{Co}_3\text{O}_4$ ,  $\text{NiO}$ ,  $\text{TiO}_2$ ,  $\text{ZrO}_2$ ,  $\text{CeO}_2$ ,  $\text{LiCoO}_2$ ,  $\text{CoFe}_2\text{O}_4$ ,  $\text{NiFe}_2\text{O}_4$ , etc. particles [5–9]. Hydrothermal method is simple to use and scale, hydrothermal reactions are performed in reactors-autoclaves, and the properties and size of particles can be controlled. At the same time, one of important shortcomings of this method is ineffective control over the aggregation of nanoparticles.

This work is concerned with the hydrothermal synthesis of  $\text{LiM}_x\text{O}_y$  and  $\text{M}_m\text{O}_n$  metal oxide nanoparticles with the use of supercritical water under continuous conditions. The procedures for performing experimental studies are described and the results obtained for the synthesized samples by scanning electron microscopy (HRTEM) and X-ray diffraction (XRD) are presented.

## EXPERIMENTAL

### *Unit and Experimental Procedures*

A scheme of the unit used for the hydrothermal synthesis of metal oxide nanoparticles is shown in Fig. 1. The unit includes a tubular flow reactor consisting of two parts, each 3 m long, with an inside diameter of 1.75 mm (the volume of the reactor is then 7.2 and 14.4 cm<sup>3</sup>), one piston pump 3, syringe pump 4, back pressure regulator 9, electrical furnace with a

boiling sand layer 7, refrigerator 8, mixer of flows 6, manometers and pressure gauges.

All the syntheses of metal oxide nanoparticles were performed using approximately the same procedure. The initial mother liquor was prepared by dissolving equi- or nonequimolar amounts of first metal ( $\text{M}_1$ ) nitrate, sulfate, or acetate and another salt of the second metal ( $\text{M}_2$ ). The mother liquor (*flow 1*) was introduced by the syringe pump into mixer 6 in a ratio of 1 : 10 or 2 : 10 with respect to supercritical water (*flow 2*) continuously supplied to the same mixture by the piston pump. Transformations were performed at temperatures and pressures close to the critical parameters of mixtures containing more than 95% water (temperature above 371°C and pressure above 230 atm). The products of the interaction of salts with supercritical water passed from the reactor into a heat exchanger and, through a back pressure regulator, into an accumulating vessel.

Depending on the size and properties of crystals formed, hydrothermal synthesis products were often a mixture of nonprecipitating particles in water. Metal oxide particles were isolated from solutions for analyzing the solid phase by solution centrifugation or evaporation followed by solid phase drying.

An important role in the hydrothermal synthesis of metal oxide nanoparticles is played by the principle and device for mixing mother liquor and supercritical water flows. On the one hand, it was shown [8, 10] that uniform mixing of two flows in the shortest contact time possible provides good reproducibility of the results and a narrow particle-size distribution in repeated experiments. On the other hand, the kinetic peculiarities of the reaction itself, the properties of particles formed, the ratio between flows, slow transport of particles from the zone of mixing of flows into

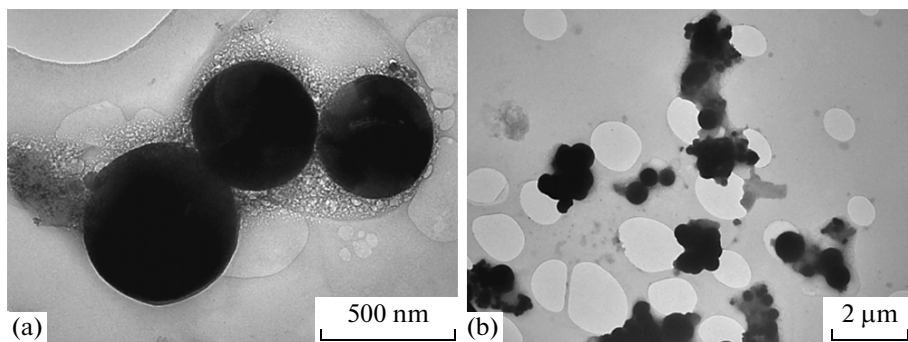


**Fig. 2.** HRTEM images of  $\text{LiCoO}_2$  particles obtained in hydrothermal synthesis.

the reactor result in the agglomeration of particles, their agglomeration on the surface of the mixer and reactor, and, eventually, blocking of reactor tubes. The creation of a universal device for mixing or a reactor for the hydrothermal synthesis of a broad class of nanoparticles is, likely, not the main goal, and studies are developing in the direction of creating mixing devices for particular classes of reactions.

In performing hydrothermal syntheses of metal oxide nanoparticles in supercritical water, the author encountered the phenomenon of fast formation of metal oxide nanoparticles ( $\text{Cd}_m\text{O}_n$  and  $\text{CuO}_2$ ) directly in the zone of mixing of flows followed by their agglomeration and blocking of reactor tubes. Clearly, additional studies are necessary for synthesizing such compounds for the creation of mixing conditions for continuous synthesis of metal oxide nanoparticles in a tubular flow reactor. For this reason, the results obtained in synthesizing these compounds are not reported in this work.

#### Sample Analysis Methods

The structure, phase, and elemental composition of the samples were analyzed by the HRTEM and XRD methods. Several aqueous products were analyzed using UV spectroscopy. The X-ray diffraction patterns were recorded on an HZG-4 (Germany) diffractometer using  $\text{CuK}\alpha$  radiation. The X-ray patterns were analyzed using the PDF base of X-ray powder data.

The transmission spectra of solutions containing nanoparticles were recorded on a UV-2501 PC (Shimadzu) spectrophotometer with an ISR-240 A diffuse reflectance accessory. The spectra were recorded with respect to a reflectance standard ( $\text{BaSO}_4$ ) over the frequency range  $11000$ – $54000$   $\text{cm}^{-1}$ . Samples in the form of solutions were placed into quartz cells with optical paths of 1, 2, and 10 mm. The data were represented in the optical density  $D$ —wave number coordinates.

#### Materials and Solutions

Solutions of precursors were prepared from pure anhydrous  $\text{LiNO}_3$ ,  $\text{CoSO}_4 \cdot 7\text{H}_2\text{O}$ ,  $\text{Fe}(\text{NO}_3)_3 \cdot 3\text{H}_2\text{O}$ ,  $\text{Ni}(\text{CH}_3\text{COO})_2 \cdot 4\text{H}_2\text{O}$ ,  $\text{Ni}(\text{NO}_3)_3 \cdot 6\text{H}_2\text{O}$ ,  $\text{Cu}(\text{CH}_3\text{COO})_2 \cdot \text{H}_2\text{O}$ ,  $\text{ZnSO}_4 \cdot 7\text{H}_2\text{O}$ ,  $\text{Ga}(\text{NO}_3)_3 \cdot 8\text{H}_2\text{O}$ , and  $\text{Ce}(\text{NO}_3)_3 \cdot 6\text{H}_2\text{O}$  salts without additional purification and doubly distilled water. The hydrothermal syntheses of (expected) oxides of two metals  $\text{LiMO}_x$  ( $\text{LiCoO}_2$ ,  $\text{LiFeO}_2$ ,  $\text{LiNiO}_2$ ,  $\text{LiZnO}_2$ , and  $\text{LiCuO}_2$ ), one of which was Li, was performed under continuous conditions in a flow reactor. The  $\text{M}_y\text{O}_x$  ( $\text{Ga}_y\text{O}_x$ ,  $\text{Cd}_y\text{O}_x$ , and  $\text{Ce}_y\text{O}_x$ ) compounds were synthesized in supercritical water using a similar procedure. The initial mother liquors for the synthesis of these compounds were prepared by the solution of one or two salts in water. A mother liquor was introduced into the reactor (*flow 1*) through a mixer, in which it was mixed with supercritical water (*flow 2*).

#### RESULTS AND DISCUSSION

##### Hydrothermal Syntheses of $\text{LiMO}_x$ Metal Oxide Nanoparticles

**The synthesis of  $\text{LiCoO}_x$ .** The hydrothermal synthesis of the  $\text{LiCoO}_2$  compound was performed using 0.1 M aqueous solutions of lithium nitrate  $\text{LiNO}_3$  and cobalt sulfate  $\text{CoSO}_4$ . The temperature and pressure of hydrothermal synthesis were  $382$ – $397^\circ\text{C}$  and  $226$ – $230$  atm. The HRTEM images of particles (hydrothermal synthesis products) are shown in Fig. 2. We see that  $\text{LiCoO}_2$  particles are round and have a size of  $\sim 500$  nm. These particles are surrounded by a coat consisting of products formed after solvent evaporation. Large ( $\sim 500$  nm) particles form agglomerates consisting of 3–4 particles, smaller particles form agglomerates of 10 and more particles.

**The synthesis of  $\text{LiFeO}_x$ .** The synthesis was performed using a 0.1 M aqueous solution of lithium nitrate  $\text{LiNO}_3$  and a 0.1 M aqueous solution of iron nitrate  $\text{Fe}(\text{NO}_3)_3$ . The temperature and pressure were  $376^\circ\text{C}$  and 230 atm. Reaction products were dark red, they precipitated with time. The X-ray pattern of dry samples did not substantiate the presence of a  $\text{LiFeO}_x$

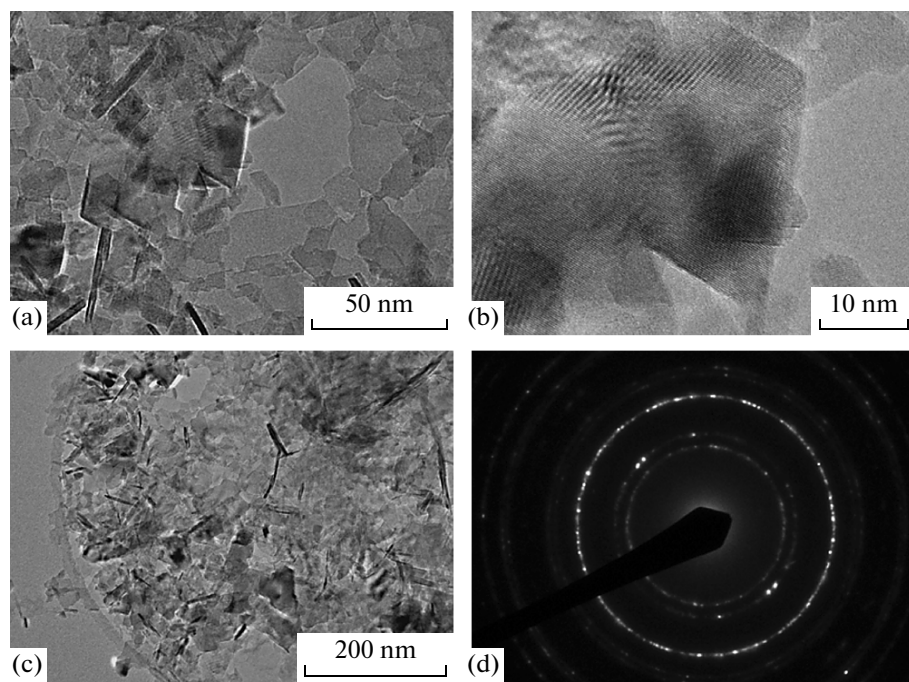


**Fig. 3.** HRTEM images of (a, b, c) synthesized  $\text{LiNiO}_2$  sample and (d) the structure of interatomic interplanar distances.

compound. Reaction products only contained the  $\alpha\text{-Fe}_2\text{O}_3$  crystalline phase and an amorphous phase.

**The synthesis of  $\text{LiNiO}_2$ .** The synthesis was performed using 0.1 M solutions of lithium nitrate  $\text{LiNO}_3$  and nickel acetate  $\text{Ni}(\text{CH}_3\text{COO})_2$ . The HRTEM image of the synthesized desired compound is shown in Fig. 3. The compound had the form of layered plates ~50 nm in size and ~2–3 nm thick. For this structure, interatomic interplanar distances were (in nm) 0.245 s, 0.210 w, 0.150 vs, 0.130 m, and 0.122 m (Fig. 3d); they corresponded to the  $\text{LiNiO}_2$  compound. The sample also contained more contrast 3–5 nm particles, for which interatomic interplanar distance (0.246 nm)

was the same as for the layered phase. The conclusion can be drawn that the layered phase is  $\text{LiNiO}_2$  (a high degree of the replacement of nickel by lithium), whereas small contrast particles with a low degree of replacement are the  $\text{NiO}$  phase. This was substantiated by the X-ray diffraction data.

**The synthesis of  $\text{LiZnO}_2$ .** The synthesis was performed using 0.1 M solutions of lithium nitrate  $\text{LiNO}_3$  and zinc sulfate  $\text{ZnSO}_4$ . The TEM image of the synthesized  $\text{LiZnO}_2$  compound is shown in Fig. 4. The product contained structures of two types: plates (characteristic size ~10 nm  $\times$  ~1  $\mu\text{m}$ ) and aggregates of isometric crystals with size no more than 10 nm. The plates were unstable, structure disordering occurred under the action of an HRTEM beam of electrons. The energy dispersive X-ray (EDX) spectra give an intense Zn line for the plates.

**The synthesis of  $\text{LiCuO}_2$ .** A mother liquor (0.1 M) was prepared by dissolving lithium nitrate  $\text{LiNO}_3$  and copper acetate  $\text{Cu}(\text{CH}_3\text{COO})_2$  in water. According to the scanning electron microscopy data, the synthesized sample was a polycrystalline mixture of well faceted crystals, which had cubic symmetry and were fairly uniform as concerns their habitus (Fig. 5). Their shapes and sizes were: isomorphic (cubes), ~50 nm; prolate (parallelepipeds), ~50  $\times$  150 nm, and flattened (plates), 50  $\times$  100 nm. Crystals formed characteristics multibranch dendrites. An amorphous molecular layer with a molecular thickness formed on the surface of crystals under the action of an HRTEM electron beam, as was characteristic of crystalline lithium compounds.

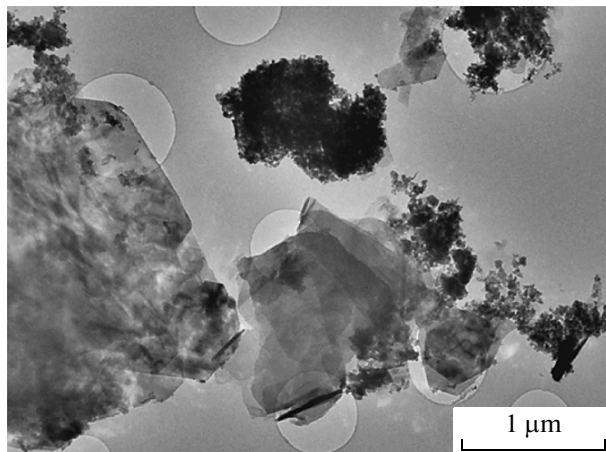


**Fig. 4.** Image of the synthesized  $\text{LiZnO}_2$  sample.

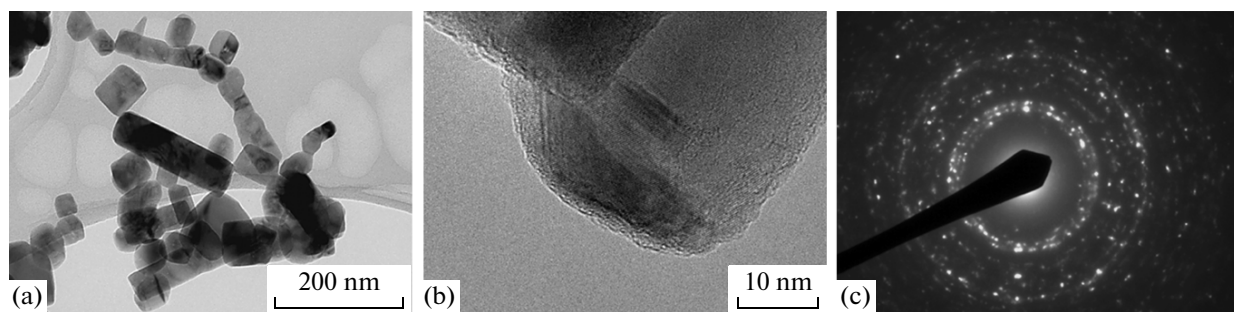


**Fig. 5.** Images of a polycrystalline mixture of  $\text{LiCuO}_2$  crystals obtained in hydrothermal synthesis.

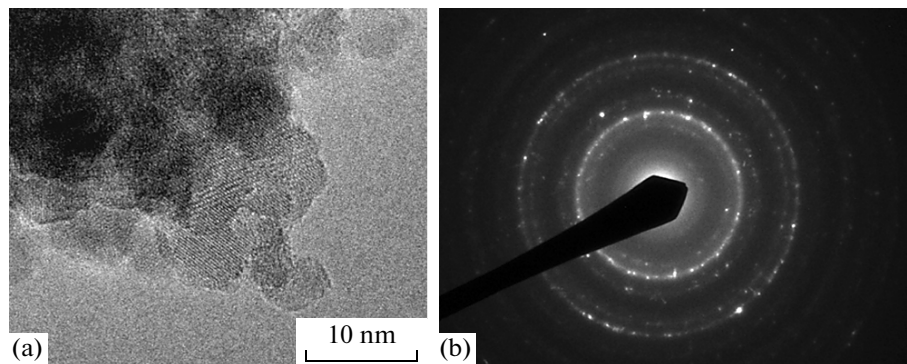


**Fig. 6.** HRTEM images of  $\gamma\text{-Ga}_2\text{O}_3$  in combination with a not identified crystalline phase.

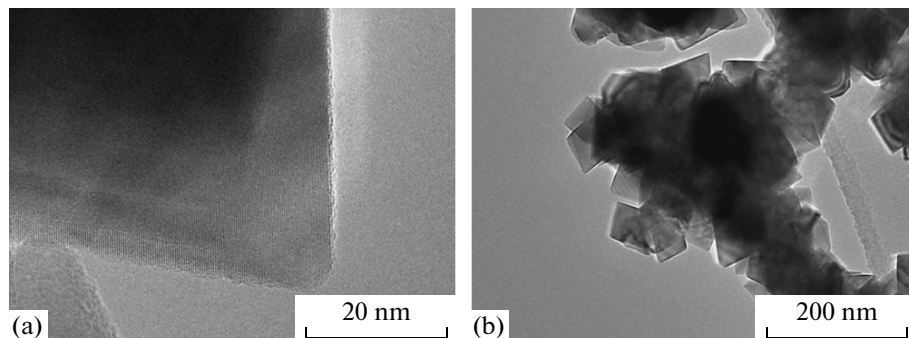


**Fig. 7.** HRTEM images of  $\text{CeO}_2$  crystals formed under hydrothermal conditions in supercritical water.

The calculated interatomic interplanar distances were (nm) 0.282 w, 0.257 m, 0.230 m, 0.175 m, 0.150 m, and 0.140 s (Fig. 5). They correspond to lithium cuprite  $\text{LiCuO}_2$  and  $\text{CuO}$ . The X-ray data also substantiate the presence of a substantial amount of  $\text{CuO}$ .

#### *The Hydrothermal Syntheses of Metal Oxide $M_y\text{O}_x$ Nanoparticles*

The hydrothermal synthesis of  $\text{Ga}_2\text{O}_3$  and  $\text{CeO}_2$  metal oxides was performed under continuous conditions in a flow reactor as described above.

**The synthesis of  $\text{Ga}_2\text{O}_3$ .**  $\text{Ga}_2\text{O}_3$  was synthesized from a 0.1 M solution of  $\text{Ga}(\text{NO}_3)_3 \cdot 8\text{H}_2\text{O}$  in water. The temperature and pressure of the reaction were 365–384°C and 235 atm. The flow rate of water (*flow 2*) was 10 ml/min, and the flow rate of the reagent (*flow 1*) was 2 ml/min. The hydrothermal reaction gave products in the form of a homogeneous dark-colored solution, which was evaporated to obtain the solid phase. According to the HRTEM data, the synthesized compound consisted of high-dispersity (2–5 nm) crystals (Fig. 6). It contained separate blocks of pseudomorphic crystals up to 100 nm in size. The calculated interatomic interplanar distances were (nm) 0.295 w, 0.250 vs, 0.230 m, 0.205 m, 0.160 m,

and 0.145 s (Fig. 6b). The X-ray diffraction data showed that the main phase in the synthesized compound was  $\gamma\text{-Ga}_2\text{O}_3$  in combination with a not identified crystalline phase.

**The synthesis of  $\text{CeO}_2$ .** The initial material was a 0.2 M solution of  $\text{Ce}(\text{NO}_3)_3 \cdot 6\text{H}_2\text{O}$  in water. The temperature of the reaction was 375–390°C, and the pressure was 260 atm. The flow rate of water (*flow 2*) was 10 ml/min, and the flow rater of the reagent (*flow 1*) was 3 ml/min. The reaction product was a whitish-yellow solution, from which a solid product gradually precipitated. According to the HRTEM data, the solid products were a homogeneous mixture of well faceted isometric crystals, whose size was ~100 nm (Fig. 7). The crystals had a dislocation block structure, and multibranch dendrites of these crystals were observed. The energy dispersive X-ray (EDX) spectra of a solution of the products gave an intense Ce line. According to the X-ray diffraction data, the main synthesized solid phase was  $\text{CeO}_2$ .

#### ACKNOWLEDGMENTS

This work was financially supported by the International Science and Technology Center, project no. 3670

and by the Russian Foundation for Basic Research (project no. 00282).

#### REFERENCES

1. E. Reverchon, and R. Adami, *J. Supercrit. Fluids* **37**, 1 (2006).
2. J. Jung and M. Perrut, *J. Supercrit. Fluids* **20**, 179 (2001).
3. Y. Zhang and C. Erkey, *J. Supercrit. Fluids* **38**, 252 (2006).
4. C. Aymonier, A. Loppiner-Serani, H. Reveron, et al., *J. Supercrit. Fluids* **38**, 242 (2006).
5. T. Adschari, Y. Hakuta, and K. Arai, *Ind. Eng. Chem. Res.* **39**, 4901 (2000).
6. T. Adschari, Y. Hakuta, K. Sue, and K. Arai, *J. Nanopart. Res.* **3**, 227 (2001).
7. A. Cabahas, J. Darr, E. Lester, and M. Poliakoff, *J. Mater. Chem.* **11**, 561 (2001).
8. T. Adshiri, S. Takami, M. Umetsu, and S. Ohara, *Ceram. Trans.* **146**, 3 (2005).
9. S. Kawasa, Y. Xiuyi, K. Sue, et al., *J. Supercrit. Fluids* **50**, 276 (2009).
10. P. J. Blood, J. P. Denyer, B. J. Azzopardi, et al., *Chem. Eng. Sci.* **59**, 2853 (2004).